

# SK2 channels regulate mitochondrial respiration and mitochondrial $\text{Ca}^{2+}$ uptake

Birgit Honrath<sup>1,2</sup>, Lina Matschke<sup>3</sup>, Tammo Meyer<sup>2</sup>, Lena Magerhans<sup>1</sup>, Fabiana Perocchi<sup>4,5</sup>, Goutham K Ganjam<sup>1</sup>, Hans Zischka<sup>6</sup>, Cornelius Krasel<sup>1</sup>, Albert Gerding<sup>7</sup>, Barbara M Bakker<sup>7</sup>, Moritz Bünemann<sup>1</sup>, Stefan Strack<sup>8</sup>, Niels Decher<sup>3</sup>, Carsten Culmsee<sup>1</sup> and Amalia M Dolga<sup>\*,1,2</sup>

Mitochondrial calcium ( $[\text{Ca}^{2+}]_m$ ) overload and changes in mitochondrial metabolism are key players in neuronal death. Small conductance calcium-activated potassium (SK) channels provide protection in different paradigms of neuronal cell death. Recently, SK channels were identified at the inner mitochondrial membrane, however, their particular role in the observed neuroprotection remains unclear. Here, we show a potential neuroprotective mechanism that involves attenuation of  $[\text{Ca}^{2+}]_m$  uptake upon SK channel activation as detected by time lapse mitochondrial  $\text{Ca}^{2+}$  measurements with the  $\text{Ca}^{2+}$ -binding mitochondria-targeted aequorin and FRET-based  $[\text{Ca}^{2+}]_m$  probes. High-resolution respirometry revealed a reduction in mitochondrial respiration and complex I activity upon pharmacological activation and overexpression of mitochondrial SK2 channels resulting in reduced mitochondrial ROS formation. Overexpression of mitochondria-targeted SK2 channels enhanced mitochondrial resilience against neuronal death, and this effect was inhibited by overexpression of a mitochondria-targeted dominant-negative SK2 channel. These findings suggest that SK channels provide neuroprotection by reducing  $[\text{Ca}^{2+}]_m$  uptake and mitochondrial respiration in conditions, where sustained mitochondrial damage determines progressive neuronal death. *Cell Death and Differentiation* (2017) 24, 761–773; doi:10.1038/cdd.2017.2; published online 10 March 2017

Under physiological conditions, mitochondrial calcium ( $[\text{Ca}^{2+}]_m$ ) uptake across the inner mitochondrial membrane is essential to drive mitochondrial metabolism and respiration, as many enzymes involved in these processes are  $\text{Ca}^{2+}$ -sensitive. Moderate increases in  $[\text{Ca}^{2+}]_m$  activate  $\text{Ca}^{2+}$ -sensitive dehydrogenases to enhance oxidative phosphorylation and ATP production, thereby maintaining the driving force for  $[\text{Ca}^{2+}]_m$  uptake and allowing for a fast adaptive response to increasing energy demands.<sup>1–3</sup> Oxidative stress in neurons leads to rapid  $\text{Ca}^{2+}$  influx through voltage-dependent channels at the plasma membrane, and to the release of  $\text{Ca}^{2+}$  from the endoplasmic reticulum (ER) through inositol-1,4,5-triphosphate receptors ( $\text{IP}_3\text{R}$ ).<sup>4–7</sup> Altogether, this facilitates an increase in intracellular  $\text{Ca}^{2+}$  and accumulation of  $[\text{Ca}^{2+}]_m$ , which induces detrimental formation of the mitochondrial permeability transition pore.<sup>8–10</sup> Further, oxidative stress-induced  $[\text{Ca}^{2+}]_m$  overload is accompanied by changes in mitochondrial metabolism, for instance alterations in ATP synthesis and NADP(H) oxidation leading to a further increase in reactive oxygen species (ROS).<sup>11,12</sup> Such  $[\text{Ca}^{2+}]_m$  overload and ROS formation are key players in neuronal cell death. In contrast, the physiological  $\text{Ca}^{2+}$  buffering capacity of mitochondria is of significant importance for neuronal function and maintenance. For instance, in the neuronal presynapse

$[\text{Ca}^{2+}]_m$  buffering contributes to the regulation of synaptic transmission,<sup>13</sup> and in the postsynaptic compartment  $[\text{Ca}^{2+}]_m$  buffering spatially modulates  $\text{Ca}^{2+}$  wave propagation when synaptic activity is increased.<sup>14</sup>

$[\text{Ca}^{2+}]_m$  buffering is tightly regulated by  $\text{Ca}^{2+}$  influx and efflux mechanisms.<sup>1,2,15</sup>  $[\text{Ca}^{2+}]_m$  influx at the inner mitochondrial membrane is mediated by the mitochondrial calcium uniporter, and  $[\text{Ca}^{2+}]_m$  efflux is mediated by the mitochondrial  $\text{Na}^+/\text{Ca}^{2+}$ -exchanger (mNCCX) and  $\text{H}^+/\text{Ca}^{2+}$  exchanger (mHCX).<sup>16–18</sup> Further, mitochondrial potassium channels may significantly contribute to the regulation of  $[\text{Ca}^{2+}]_m$  buffering and related metabolic functions of mitochondria, thereby, determining neuronal functionality and survival.

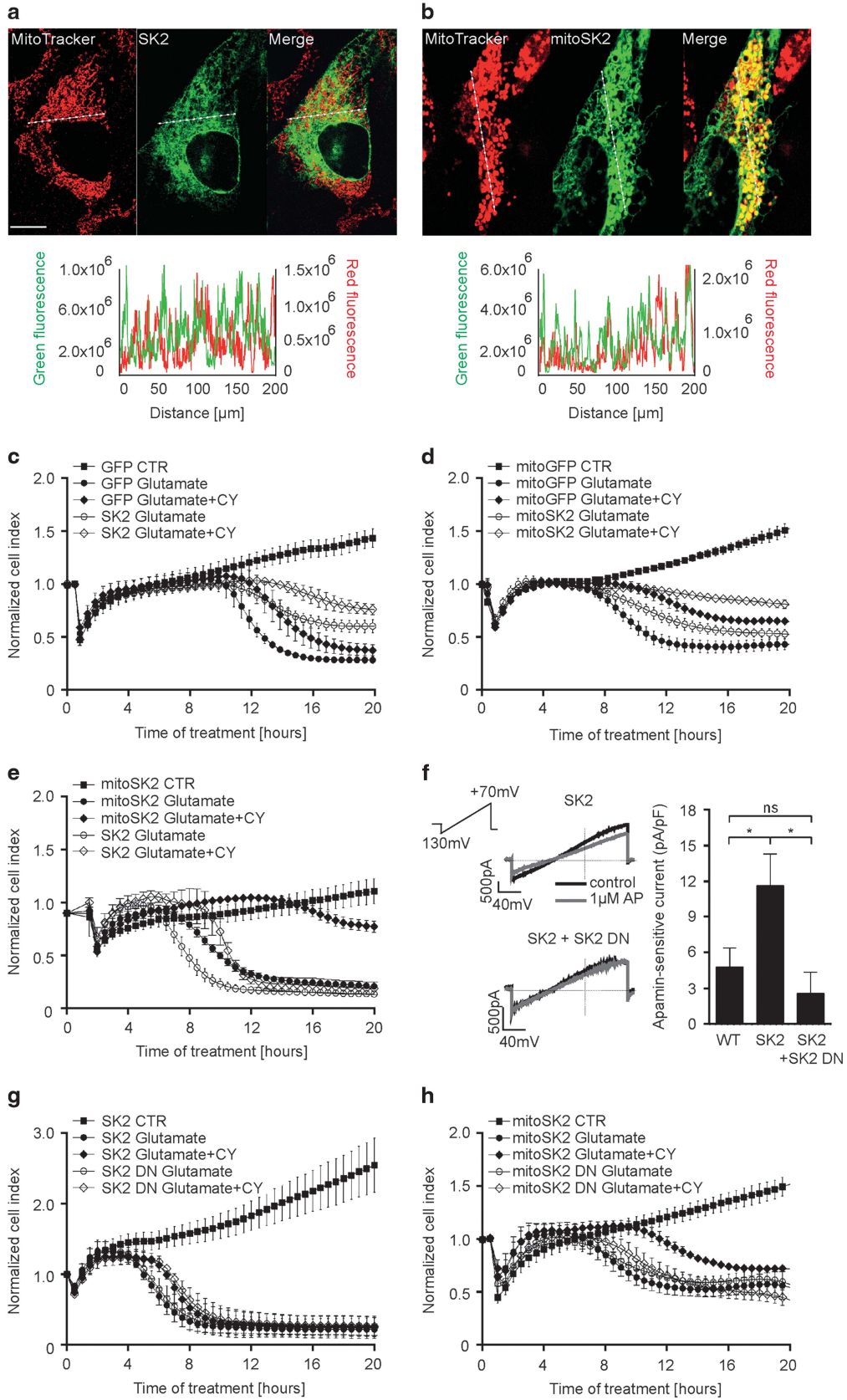
Recently, small conductance calcium-activated potassium channels (KCNN/SK/ $\text{K}_{\text{Ca}}$ ), in particular the SK2 and SK3 channel subtypes, were identified at the inner mitochondrial membrane of neuronal and cardiac cells.<sup>19–21</sup> Dysfunction of potassium channels has been implicated in the pathogenesis of psychiatric disorders and neurodegenerative diseases such as schizophrenia and Alzheimer's disease or Parkinson's disease, respectively.<sup>22–24</sup>

At the plasma membrane, SK channels reside in close proximity to NMDA receptors and mediate after-hyperpolarization thereby reducing neuronal excitability. Positive

<sup>1</sup>Institute of Pharmacology and Clinical Pharmacy, University of Marburg, Marburg, Germany; <sup>2</sup>Faculty of Science and Engineering, Groningen Research Institute of Pharmacy, Behavioural and Cognitive Neurosciences (BCN), Department of Molecular Pharmacology, University of Groningen, Groningen, The Netherlands; <sup>3</sup>Institute of Physiology and Pathophysiology, Vegetative Physiology, University of Marburg, Marburg, Germany; <sup>4</sup>Gene Center/Department of Biochemistry, Ludwig-Maximilians Universität München, Munich, Germany; <sup>5</sup>Institute for Obesity and Diabetes, Helmholtz Zentrum München, Neuherberg, Germany; <sup>6</sup>Institute of Molecular Toxicology and Pharmacology, Helmholtz Center Munich, German Research Center for Environmental Health GmbH, Neuherberg, Germany; <sup>7</sup>Center for Liver, Digestive and Metabolic Diseases, Department of Pediatrics & Systems Biology Center for Energy Metabolism and Ageing, University of Groningen, University Medical Center Groningen, Groningen, The Netherlands and <sup>8</sup>Department of Pharmacology, University of Iowa Carver College of Medicine, Iowa City, IA, USA

\*Corresponding author: A Dolga, Faculty of Science and Engineering, Groningen Research Institute of Pharmacy, Department of Molecular Pharmacology, University of Groningen, Antonius Deusinglaan 1, Groningen, The Netherlands. Tel: +31 50 363 6372; Fax: +31 50 363 6908; E-mail: a.m.dolga@rug.nl

Received 05.7.16; revised 29.11.16; accepted 14.12.16; Edited by S Fulda; published online 10.3.2017



pharmacological SK channel modulation using CyPPA or NS309 protected neuronal cells in different paradigms of cell death triggered by H<sub>2</sub>O<sub>2</sub>, glutamate,<sup>21,25</sup> or ER stress<sup>26</sup> *in vitro*, and in models of cerebral ischemia *in vivo*.<sup>20,27–29</sup> Importantly, the observed protection of neuronal cells was not exclusively conferred by reducing the excitability of the plasma membrane.<sup>20,30</sup> Rather, SK channel activation by CyPPA preserved mitochondrial integrity by restoring the mitochondrial membrane potential (MMP), reducing mitochondrial ROS formation and preventing organelle fragmentation in paradigms of oxidative stress.<sup>21</sup>

So far, most studies investigated the neuroprotective potential of SK channels at the plasma membrane in cell death models related to neuronal excitability or ischemia. However, little is known about their distinct function in mitochondria in conditions of oxidative stress. In this study, we investigated the impact of mitochondrial SK2 channels in a model of oxidative glutamate toxicity, also termed oxytosis, in neuronal HT22 cells. In these cells, glutamate induces cell death by oxidative stress that is independent of NMDAR activation.<sup>31</sup> We show that the activation of mitochondrial SK2 channels is a major determinant in the protection against oxytosis by a mechanism involving the regulation of mitochondrial respiration and mitochondrial Ca<sup>2+</sup> uptake.

## Results

**Targeted expression of SK2 channels at the mitochondria enhances CyPPA-mediated protection against glutamate toxicity.** The applied model system of HT22 cells is deficient in SK3 channels.<sup>21</sup> In order to distinguish between SK2 channel-mediated effects at the plasma membrane and those at the inner mitochondrial membrane, HT22 cells were transfected with plasmids encoding for non-targeted SK2 channels (SK2), mitochondrial SK2 channels (mitoSK2) and corresponding control plasmids GFP or mitoGFP with a transfection efficiency of 60–80% (Supplementary Figure S1A). In contrast to non-targeted SK2 showing a diffuse cellular distribution (Figure 1a), transfection with mitoSK2 resulted in a strong co-localization with the mitochondria (Figure 1b).

As shown by impedance-based measurements,<sup>32</sup> application of CyPPA alone did not alter cell growth irrespective of the transfected SK2 plasmids (Supplementary Figure S1B and C). In previous studies, CyPPA exerted sustained protection against glutamate toxicity at concentrations higher than 20 μM.<sup>21</sup> Therefore, we used lower concentrations (10 μM) to induce transient protection. Overexpression of GFP or non-targeted SK2 and glutamate treatment showed cell death ~8–

10 h after onset of glutamate exposure (Figure 1c), and CyPPA delayed cell death as detected by a right shift in the cellular impedance curves. Cells overexpressing mitoSK2 showed delayed cell death during glutamate treatment compared to cells overexpressing mitoGFP, and a prolonged protection when treated with CyPPA (Figure 1d). Notably, mitoSK2 overexpression delayed glutamate-induced cell death compared to non-targeted SK2 expression, and only mitoSK2 overexpression fully protected cells against glutamate when co-treated with CyPPA (Figure 1e).

Next, we assessed the effects of overexpression of a dominant-negative SK2 channel mutant (non-targeted or mitochondrial) on cell viability during the glutamate challenge (SK2 DN; mitoSK2 DN). To determine SK channel-encoded currents in native cells and cells overexpressing functional or dominant-negative SK2 channels, the selective SK channel inhibitor apamin<sup>33</sup> was used. Cells transfected with SK2 showed an increased apamin-sensitive current compared to wildtype control cells (Figure 1f). SK2 DN significantly reduced the apamin-sensitive current in native and SK2-transfected cells. The subcellular localization of non-functional SK2 DN and mitoSK2 DN was confirmed by immunofluorescence (Supplementary Figure S1D). Further, the dominant-negative mutants did not alter cell proliferation in the presence or absence of CyPPA (Supplementary Figure S1E and F). Cells overexpressing SK2 DN showed a negligible reduction of CyPPA-mediated protection against oxidative glutamate toxicity compared to control SK2-overexpressing cells (Figure 1g). On the contrary, overexpression of mitoSK2 DN greatly compromised CyPPA-mediated protection compared to mitoSK2 overexpression (Figure 1h).

Further, overexpression of mitoSK2, but not non-targeted SK2, significantly enhanced CyPPA-mediated preservation of cellular ATP levels during the glutamate challenge compared to the corresponding GFP controls (Supplementary Figure S2A and B). Cells overexpressing mitoSK2 DN showed reduced cellular ATP levels compared to mitoSK2, while overexpression of SK2 DN failed to impair CyPPA-mediated protection against oxidative glutamate toxicity compared to SK2 as a control (Supplementary Figure S2C and D). Direct comparison revealed that mitochondrial SK2 channels conferred an additive effect to the pharmacological activation compared to non-targeted SK2 channels (Supplementary Figure S2E), which supports the conclusion that protection was mediated by the mitochondrial SK2 channels.

Further, CyPPA-induced protection against oxytosis was independent of extracellular calcium. Co-treatment of HT22 cells with CyPPA and glutamate in medium supplemented with

**Figure 1** Overexpression of mitochondrial SK2 channels enhances CyPPA-mediated protection against glutamate-induced cell death. (a, and b) Representative confocal images of HT22 cells overexpressing (a) non-targeted GFP-tagged SK2 channel or (b) mitochondrial SK2 channel co-localizing with mitochondria (MitoTracker Red) ( $n = 10–15$  cells/plasmid). Lower panels: plot profile of GFP and MitoTracker Red along the dashed line. Scale bars: 10 μm. (c–e) xCELLigence measurement of cell viability during glutamate exposure in the presence or absence of CyPPA (CY) in cells overexpressing (c) GFP control and SK2, (d) mitoGFP control and mitoSK2, or (e) SK2 and mitoSK2 (mean ± SD,  $n = 6–8$ ). (f) Electrophysiological recordings of apamin-sensitive currents in HT22 cells transfected with the SK2 alone or SK2 combined with SK2 DN before and after application of 1 μM apamin (AP). Left panel: representative whole-cell currents. Right panel: quantification of apamin-sensitive currents. Data are shown as mean ± SEM,  $n = 6$ , paired Student's *t*-test, \* $P < 0.05$ , ns not significant. (g and h) xCELLigence measurement of cell viability during glutamate exposure in the presence or absence of CyPPA (CY) in cells overexpressing (g) SK2 and SK2 DN, or (h) mitoSK2 and mitoSK2 DN (mean ± SD,  $n = 6–8$ )

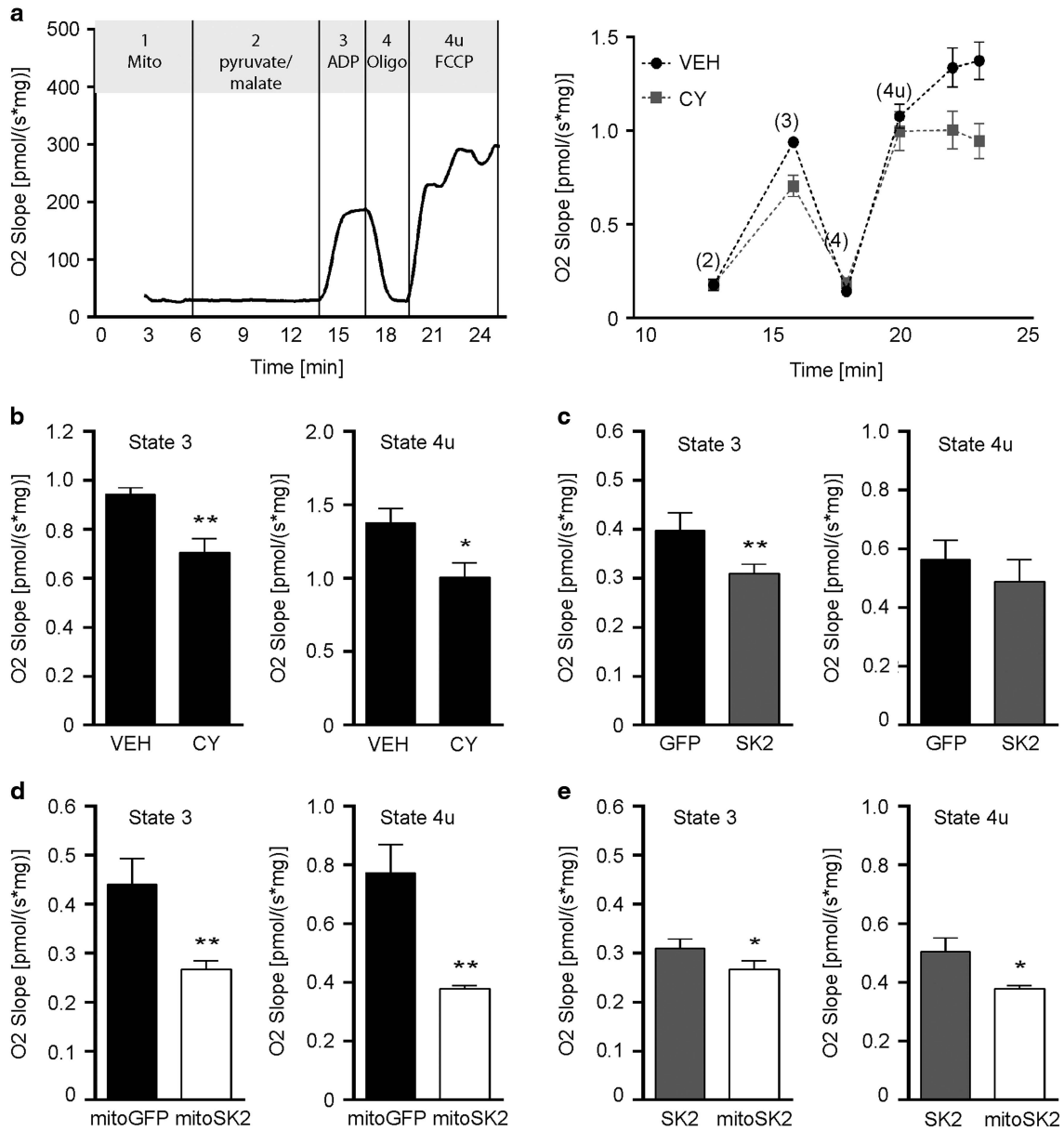


**Figure 2** Overexpression of mitochondrial SK2 channels attenuates mitochondrial respiration. (a) Representative oxygen slope of isolated mitochondria from HT22 cells. Left panel: definition of mitochondrial states (1, 2, 3, 4, 4u) by addition of indicated substances in a representative measurement. Right panel: corrected oxygen slope showing mitochondrial states after treatment with vehicle (VEH) or CyPPA (CY). Mitochondrial states are indicated as (2–4u). (b–e) Quantification of state 3 (left panels) and state 4u (right panels) of mitochondria pre-treated with vehicle (VEH) or CyPPA (CY) (b), of HT22 cells overexpressing GFP or SK2 (c), mitoGFP or mitoSK2 (d), or SK2 or mitoSK2 (e). Data are shown as mean  $\pm$  SD,  $n = 3–5$ , \* $P < 0.05$ , \*\* $P < 0.01$  compared to indicated control

different EGTA concentrations (Supplementary Figure S3A and B), calcium-free medium (Supplementary Figure S3C) or calcium-free medium supplemented with 0.25 mM EGTA (Supplementary Figure S3D) prevented cell death strengthening the view that CyPPA-conferred protection against oxidative glutamate toxicity is largely independent of SK channels localized in the plasma membrane.

These results show that the mitochondrial SK2 channels exerted the observed protective effects, while (non-targeted) SK channels at the plasma membrane had only minor effects in this paradigm of oxidative cell death.

**MitoSK2 channels attenuate mitochondrial respiration in HT22 cells.** We next assessed whether pre-activation or overexpression of mitochondrial SK2 channels influenced mitochondrial oxidative phosphorylation (OXPHOS) in isolated mitochondria (Figure 2a). We found that CyPPA reduced the complex I-linked respiration rate in the presence of ADP (state 3; basal respiration) (Figure 2b). Moreover, the respiration rate in the presence of the uncoupling protonophore FCCP was reduced in mitochondria pre-treated with CyPPA compared to controls (state 4u). Overexpression of non-targeted SK2 reduced the state 3 mitochondrial



respiration rate compared to GFP control, while the state 4u respiration rate was comparable between these groups (Figure 2c). On the contrary, mitoSK2 overexpression reduced both mitochondrial state 3 and state 4u compared to overexpression of mitoGFP (Figure 2e). In comparison to non-targeted SK2, mitoSK2 reduced mitochondrial state 3 and state 4u respiration (Figure 2e).

Collectively, these data demonstrate that SK2 channel activation and enrichment of mitochondrial SK2 channels reduced mitochondrial respiration.

**MitoSK2 channels augment CyPPA-mediated preservation of mitochondrial integrity.** Neuronal glutamate exposure impairs mitochondrial integrity causing loss of the MMP, increases in mitochondrial ROS formation, mitochondrial calcium ( $[Ca^{2+}]_m$ ) overload and subsequent cellular ATP depletion.<sup>34</sup>

In line with previous studies,<sup>21</sup> we found that wildtype HT22 cells co-treated with glutamate and CyPPA showed reduced MMP loss (Figure 3a and Supplementary Figure S4A), reduced mitochondrial ROS formation (Figure 3e and Supplementary Figure S4B) and reduced  $[Ca^{2+}]_m$  levels (Figure 4a and Supplementary Figure S4C). Overexpression of SK2 did not accelerate the observed protective effect of CyPPA on MMP loss (Figure 3b), ROS formation (Figure 3f) or  $[Ca^{2+}]_m$  levels (Figure 4b) compared to GFP-expressing cells. On the contrary, overexpression of mitoSK2 reduced glutamate-induced mitochondrial ROS formation (Figure 3g) compared to mitoGFP-expressing cells in the presence of CyPPA. Interestingly, cells overexpressing mitoSK2 compared to mitoGFP showed lower mitochondrial ROS and  $[Ca^{2+}]_m$  levels when treated with CyPPA under basal conditions demonstrating that mitoSK2 overexpression specifically enhanced the protective effect of CyPPA on mitochondrial integrity. In line with these findings, mitoSK2 overexpressing cells showed reduced ROS and  $[Ca^{2+}]_m$  levels independent of the treatment compared to SK2 overexpressing cells (Figures 3d, h and 4d).

To investigate whether CyPPA also affected parameters upstream of mitochondrial damage, we analyzed changes in lipid peroxidation 8 h after onset of the glutamate challenge, that is, before mitochondrial damage becomes detectable.<sup>35</sup> Exposure of wildtype HT22 cells to glutamate induced a large increase in lipid peroxidation (Figure 5a and Supplementary Figure S4D). CyPPA co-treatment minimally reduced lipid peroxidation, while the 12/15-lipoxygenase (12/15-LOX) inhibitor PD146176 (refs 35,36) fully attenuated it. Overexpression of neither non-targeted SK2 channels (Figure 5b), nor mitoSK2 channels (Figure 5c) altered the glutamate-induced increase in lipid peroxidation or PD146176-mediated protection.

Taken together, we show that targeted expression of SK2 channels in the mitochondria enhanced CyPPA-mediated protection against oxidative glutamate toxicity compared to wildtype HT22 cells, mitoGFP-transfected cells and, notably, also compared to non-targeted SK2 plasmid transfected cells.

**SK2 channel activation attenuates  $[Ca^{2+}]_m$  uptake in HT22 cells.** Next, we investigated the direct effects of SK

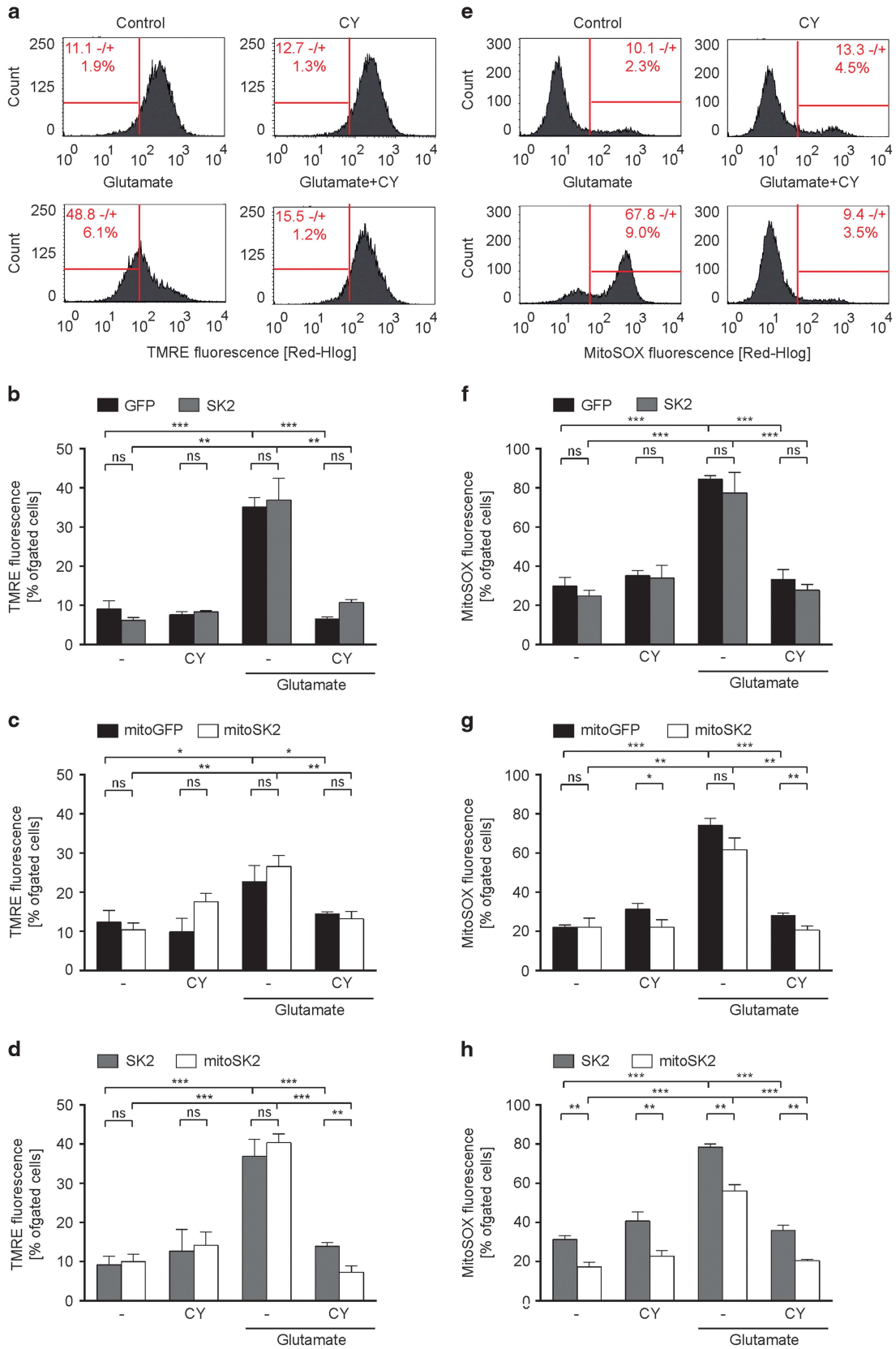
channel modulation on  $[Ca^{2+}]_m$  uptake using mitochondrial aequorin<sup>37</sup> including different stimuli to mobilize  $Ca^{2+}$ .

HT22 cells stably transfected with mitochondrial aequorin (HT22[mtAEQ]) were pre-incubated with CyPPA and apamin, respectively. ATP and carbachol-stimulated  $IP_3R$ -signaling in HT22[mtAEQ] cells showed typical kinetics of  $[Ca^{2+}]_m$  uptake as recorded in real-time after onset of the respective stimuli (Figure 6a and Supplementary Figure S5A).<sup>4,37,38</sup> The uptake of  $[Ca^{2+}]_m$  was quantified as the  $[Ca^{2+}]_m$  peak amplitude in response to ATP and carbachol stimulation. As a positive control, cells were pre-treated with KB-R7943, a blocker of the reverse mode  $Na^+/Ca^{2+}$  exchanger (mNXC),<sup>30</sup> which was shown to prevent  $[Ca^{2+}]_m$  uptake in HeLa cells.<sup>39</sup> The complex III inhibitor antimycin A served as a further positive control for  $[Ca^{2+}]_m$  uptake inhibition.<sup>40</sup> Pre-treatment with either KB-R7943 or antimycin A reduced the peak amplitude after stimulation with ATP or carbachol (Figure 6b and Supplementary Figure S5B). Furthermore, both substances also prevented glutamate-induced cell death, as measured by the MTT assay (Supplementary Figure S6A and B).

Pre-treatment with CyPPA reduced the  $[Ca^{2+}]_m$  peak amplitude following ATP application (Figure 6c), and also in conditions of carbachol-induced  $IP_3R$ -dependent  $[Ca^{2+}]_m$  uptake (Supplementary Figure S5C).<sup>4</sup> Inhibition of endogenous SK channels with apamin alone did not alter glutamate-induced cell death (Supplementary Figure S6C) or the ATP-induced  $[Ca^{2+}]_m$  peak amplitude (Figure 6d). However, apamin blocked CyPPA-mediated effects on the ATP-induced  $[Ca^{2+}]_m$  peak amplitude and provoked an increase in the  $[Ca^{2+}]_m$  peak amplitude compared to control cells. Following carbachol treatment, neither apamin alone nor combined with CyPPA changed the  $[Ca^{2+}]_m$  peak amplitude (Supplementary Figure S5D).

Quinine, an inhibitor of the mitochondrial proton/potassium exchanger (mKHE),<sup>41</sup> reduced the  $[Ca^{2+}]_m$  peak amplitude upon stimulation with ATP and carbachol (Figure 6e and Supplementary Figure S5E). In response to ATP, quinine enhanced the effect of CyPPA as the  $[Ca^{2+}]_m$  peak amplitude was slightly more reduced than with CyPPA alone. Interestingly, lowered cell viability and inhibited CyPPA-mediated protection in a model of ER stress,<sup>26</sup> while the protective effect of CyPPA against oxidative glutamate toxicity remained unchanged (Supplementary Figure S6D). HT22[mtAEQ] cells were further treated with glibenclamide (Figure 6f), an inhibitor of the ATP-dependent potassium channel ( $K_{ATP}$ ),<sup>41,42</sup> which was previously shown to reduce ATP-induced  $[Ca^{2+}]_m$  uptake.<sup>43</sup> However, in response to carbachol (Supplementary Figure S6F), glibenclamide did not reduce the  $[Ca^{2+}]_m$  peak amplitude. Notably, glibenclamide treatment rendered no protection against glutamate-induced cell death (Supplementary Figure S6E), and did not attenuate CyPPA-mediated protection against glutamate toxicity in HT22 cells.<sup>21</sup> These findings suggest that inhibition of mKHE or  $K_{ATP}$  channels did not affect SK channel-mediated effects on  $[Ca^{2+}]_m$  uptake.

Together, our results demonstrate that SK channel activation reduced the  $[Ca^{2+}]_m$  peak amplitude, thus  $[Ca^{2+}]_m$  uptake, in response to ATP and carbachol-induced  $IP_3R$ -dependent ER- $Ca^{2+}$  release into mitochondria.



**SK channel activation reduces  $[Ca^{2+}]_m$  uptake in response to glutamate and ATP in primary cortical neurons.** Next, we sought to verify our findings of SK channel-mediated modulation of  $[Ca^{2+}]_m$  uptake in primary cortical neurons (PCN). Therefore, we performed quantitative single cell analysis of basal  $[Ca^{2+}]_m$  and agonist-stimulated rises in  $[Ca^{2+}]_m$  in PCN using the mitochondria-targeted cameleon FRET sensor (Figure 7a).<sup>44,45</sup>

Glutamate initiated a rapid increase in FRET in the range of seconds, indicated by an increase in  $F_{YFP}/F_{CFP}$ , (Figure 7b) which reflects an increase in  $[Ca^{2+}]_m$  uptake. Pre-treatment of PCN with the positive control KB-R7943 reduced  $[Ca^{2+}]_m$  levels during the glutamate exposure. Pre-treatment with the SK channel activator CyPPA also resulted in a fast response similar to glutamate treatment. The initial increase in FRET was delayed and a lower FRET signal was maintained throughout the measurement showing a reduction of  $[Ca^{2+}]_m$  levels compared to glutamate treatment. SK channel inhibition

by apamin caused an accelerated onset kinetic in response to glutamate, and the FRET signal was maintained at high-levels throughout the measurement depicting highly increased  $[Ca^{2+}]_m$  levels. MK801, an NMDA receptor antagonist, also reduced mitochondrial calcium uptake in response to glutamate. Compared to CyPPA, the MK801-induced decline in mitochondrial calcium was delayed. Both, SK channel activation by CyPPA and NMDA receptor inhibition by MK801 decreased glutamate-induced calcium rises and oscillations in the cytosol with comparable kinetics (Figure 7d) indicating a possible interdependence between changes in cytosolic and in mitochondrial calcium. Thus, SK channel activation reduced  $[Ca^{2+}]_m$  uptake while its inhibition rapidly increased the uptake in response to glutamate.

Compared to glutamate, ATP treatment resulted in a slower initial increase in  $[Ca^{2+}]_m$  uptake and a less pronounced response that was not maintained throughout the measurement (Figure 7c). Instead, maximal  $[Ca^{2+}]_m$  levels were

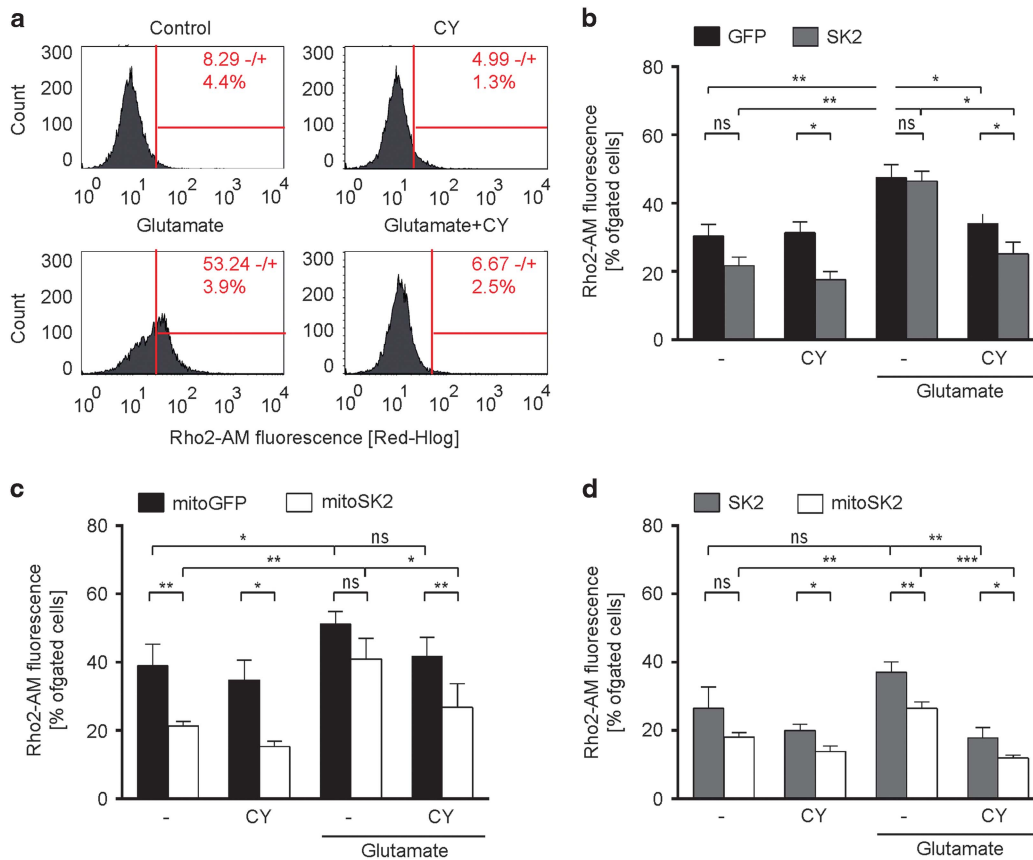


**Figure 4** SK channel activation and overexpression of mitochondrial SK2 channels decreases glutamate-induced accumulation of mitochondrial calcium. Representative measurements of mitochondrial calcium levels following glutamate exposure (16 h) in the presence or absence of CyPPA (CY), in (a) wildtype HT22 cells or HT22 cells overexpressing (b) GFP versus SK2, (c) mitoGFP versus mitoSK2, and (d) SK2 versus mitoSK2. Data are presented as mean ± SD,  $n=3$ , \* $P<0.05$ , \*\* $P>0.01$ , \*\*\* $P<0.001$

**Figure 3** Targeted overexpression of SK2 channels in the mitochondria augments CyPPA-mediated preservation of mitochondrial integrity. Mitochondrial integrity was analyzed by means of fluorescent-activated cell sorting using fluorescent probes for mitochondrial membrane potential (a-d) or mitochondrial ROS formation (e-h) following glutamate exposure (16 h) in the presence or absence of CyPPA (CY) in wildtype HT22 cells (a, e), and HT22 cells overexpressing (b, f) GFP versus SK2, (c, g) mitoGFP versus mitoSK2, and (d, h) SK2 versus mitoSK2. Data are presented as mean ± SD,  $n=3$ , \* $P<0.05$ , \*\* $P>0.01$ , \*\*\* $P<0.001$

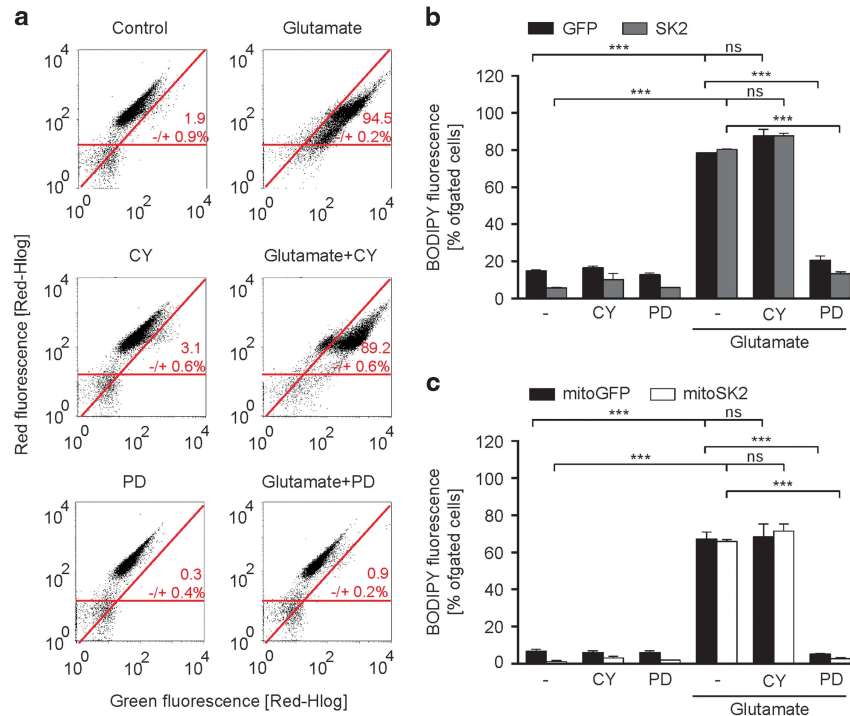


**Figure 5** Lipid peroxidation precedes CyPPA-mediated mitoprotection. Representative measurements of lipid peroxidation following glutamate exposure (8 h) in the presence or absence of CyPPA (CY) and PD146176 (PD) in (a) wildtype HT22 cells, (b) cells transfected with GFP versus SK2 or (c) mitoGFP versus mitoSK2. Results are shown as mean  $\pm$  SD,  $n=3$ , \* $P<0.05$ , \*\* $P>0.01$ , \*\*\* $P<0.001$

reached within 20 s following ATP application and nearly returned to basal levels afterwards. In response to ATP,  $[Ca^{2+}]_m$  levels were lower in cells pre-treated with the SK channel activator NS309, and higher in cells pre-treated with the SK channel inhibitor apamin. In line with our previous findings, pre-treatment with KB-R7943 reduced the FRET signal. Interestingly, in the early phase of ATP application, pre-treatment with KB-R7943 and NS309 delayed  $[Ca^{2+}]_m$  uptake and the FRET signal was maintained at low-levels. While the variation in the response to glutamate was quite small, ATP-induced responses showed a high-variability, thus not revealing overall significant differences in  $[Ca^{2+}]_m$  uptake in the presence of SK channel modulators. However, SK channel activation reduced the magnitude of  $[Ca^{2+}]_m$  uptake in the early phase of ATP stimulation, which was in line with the results from glutamate stimulation.

Taken together, our data suggest that SK channel activation is involved in the regulation of  $[Ca^{2+}]_m$  uptake in conditions of glutamate-induced oxidative stress, excitotoxicity, and ATP-induced increases in  $[Ca^{2+}]_m$  levels.

## Discussion

In the present study, we show that mitochondria-targeted SK2 channels preserved mitochondrial integrity by a mechanism involving the regulation of mitochondrial respiration and  $[Ca^{2+}]_m$  uptake in models of oxidative glutamate toxicity in a neuronal cell line and glutamate-induced excitotoxicity in primary cortical neurons.

Using mitoSK2 overexpressing cells, we delineated effects of mitochondrial SK2 channels independent of those elicited by SK2 channels at the plasma membrane. We show that mitoSK2 overexpression enhanced CyPPA-mediated protection, delayed cell death and preserved cellular ATP levels compared to control cells. In addition, overexpression of mitoSK2 further enhanced this protection compared to non-targeted SK2 overexpression suggesting a stronger impact of mitochondrial SK2 channels on cell viability after the onset of oxytosis.

In a previous study, the effect of SK2 inhibitory peptides and/or SK2 RNA interference on cell viability was assessed in HT22 cells challenged with glutamate.<sup>21</sup> Our work reveals that overexpression of a mitochondria-targeted dominant-negative SK2 channel mutant reversed the CyPPA-mediated effects on cell viability and on cellular ATP levels. In contrast, functional overexpression of a non-targeted SK2 DN mutant failed to attenuate CyPPA-mediated protection. Altogether with the fact that glutamate-induced cell death in conditions of extracellular  $Ca^{2+}$  depletion was still prevented by SK channel activation, we therefore suggest that protection against oxidative glutamate toxicity is mainly conferred by activation of mitochondrial SK2 channels.

Inhibition of complex I of the respiratory chain by high concentrations of rotenone induced cell death in human dopaminergic neurons which was restored by SK channel activation through mitochondrial conservation.<sup>20</sup> However, it is not entirely understood which mitochondrial respiratory complex is affected by SK channel activation. How disturbance of oxidative phosphorylation (OXPHOS) leads to a sustained



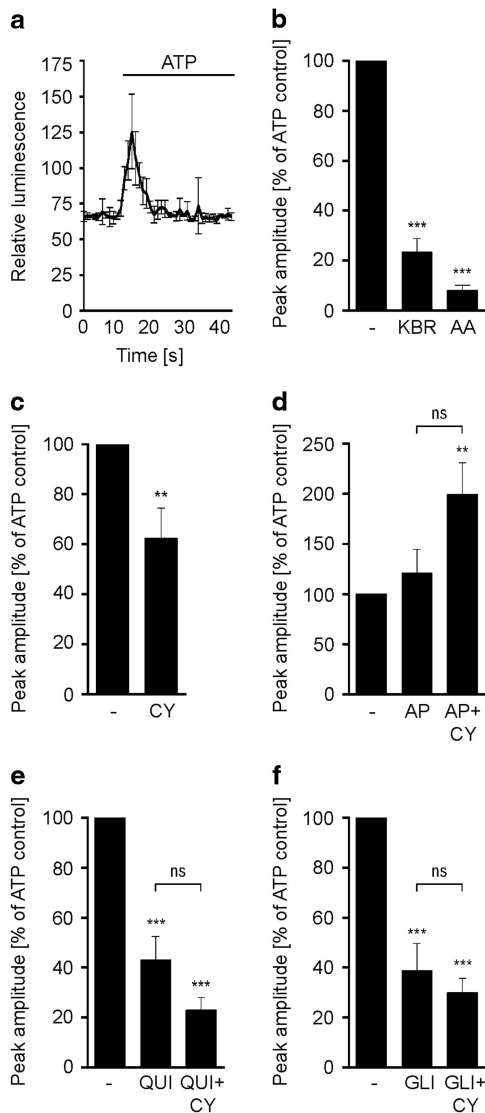


**Figure 6** SK2 channel activation reduces ATP-dependent mitochondrial calcium uptake in HT22 cells. (a) Mitochondrial calcium uptake kinetics in HT22[mtAEQ] cells stimulated with ATP. (b–f) ATP-induced changes in mitochondrial calcium uptake in cells pre-treated with (b) KB-R7943 (KBR) and antimycin A (AA), (c) CyPPA (CY), (d) apamin (AP), (e) quinine (QUI) and (f) glibenclamide (GLI). In (d–f), CyPPA co-treatment was included. Data are calculated as peak amplitude (% of control) and presented as mean  $\pm$  SEM,  $n = 6$ –8. \* $P < 0.05$ , \*\* $P < 0.01$ , \*\*\* $P < 0.001$  compared to control, ns not significant

MMP could be explained by an inhibition of mitochondrial complex V. Complex V inhibition allows a decrease in ATP production and no change in FCCP-induced mitochondrial respiration. However, activation of SK channels did not result in complex V inhibition as ATP levels were not attenuated and mitochondrial respiration was still increased. Analysis of OXPHOS in isolated mitochondria from HT22 cells revealed that CyPPA reduced the complex I-linked ADP coupled (state 3) respiration and the maximal uncoupled respiration. While complete inhibition of complex I by high-rotenone concentrations was toxic, the partial reduction in mitochondrial respiration by CyPPA was protective in our study. This corresponds to previous findings showing that at low

concentrations, which induce partial complex I inhibition, rotenone protected against glutamate toxicity in HT22 cells.<sup>46</sup> In addition, mitoSK2 overexpression also attenuated ADP coupled and uncoupled respiration compared to overexpression of GFP or SK2 as controls without exerting toxic effects. Thus, we suggest a direct link between the neuroprotective mitoSK2 overexpression and the observed decrease in respiration. This conclusion is strongly supported by detailed analysis of mitochondrial endpoints following the glutamate challenge. In fact, overexpression of mitoSK2 further enhanced CyPPA-induced protection against MMP loss, ROS formation and reduced  $[Ca^{2+}]_m$  overload compared to non-targeted SK2 overexpression. This finding corresponds to previous studies showing that a reduced function of the mitochondrial electron transport chain is accompanied with a decrease in ROS formation.<sup>47</sup>

In cultured primary neurons, activation of SK channels protected against glutamate-induced excitotoxicity by reducing NMDAR-mediated accumulation of intracellular  $Ca^{2+}$ .<sup>48</sup> In this study, we show that glutamate also triggered  $[Ca^{2+}]_m$  uptake, which was blocked by SK channel activation. Further, pre-treatment with CyPPA decreased  $[Ca^{2+}]_m$  uptake in response to ATP or IP<sub>3</sub>R-dependent signaling indicating a direct impact of mitoSK2 channel modulation on  $[Ca^{2+}]_m$  regulation.

Inhibition of KHE and  $K_{ATP}$  at the ER attenuated CyPPA-mediated effects in a model of Brefeldin A-induced ER stress indicating an essential role for proton uptake and release in the protective mechanisms observed against ER stress.<sup>26</sup> In this study, mKHE and  $K_{ATP}$  channel inhibition did not affect the CyPPA-mediated reduction in  $[Ca^{2+}]_m$  uptake in response to ATP. Thus, activation of mitochondrial SK2 channels protected against oxidative glutamate toxicity independent of other channels involved in proton flux across the inner mitochondrial membrane. This was further confirmed in rat primary neurons, where pharmacological activation of SK channels rapidly reduced  $[Ca^{2+}]_m$  uptake in response to glutamate and ATP. Although, SK channels also influenced NMDAR-mediated  $Ca^{2+}$  influx and excitotoxicity in PCN, the obtained results overall confirm our findings from the aequorin measurements showing that SK channel modulation was linked to  $Ca^{2+}$  uptake into mitochondria. This conclusion is further supported by the fact that CyPPA-mediated protection of mitochondria was independent of extracellular  $Ca^{2+}$  in HT22 cells.

As  $[Ca^{2+}]_m$  uptake primarily depends on an intact mitochondrial membrane potential,<sup>49,50</sup> the reduced mitochondrial respiration, and therefore the reduced MMP observed after SK channel activation and/or overexpression in the mitochondria may directly affect  $[Ca^{2+}]_m$  uptake and mitochondrial ROS formation. Similar to our findings on SK channel activation in the mitochondria, pharmacological activation of mitochondrial  $B_{KCa}$  channels was shown to protect against ischemia reperfusion by reducing ROS formation and  $[Ca^{2+}]_m$  uptake in rat and guinea pig heart,<sup>51,52</sup> and against ischemic injury in guinea pig heart by reducing the MMP and  $[Ca^{2+}]_m$  uptake. In line with mitochondrial  $B_{KCa}$  channels, an increased activity of mitochondrial  $I_{KCa}$  channels has also been linked to changes in MMP and  $[Ca^{2+}]_m$  levels,<sup>53</sup> which corresponds to our findings on the influence of mitoSK2 channels on mitochondrial respiration and  $[Ca^{2+}]_m$  homeostasis.

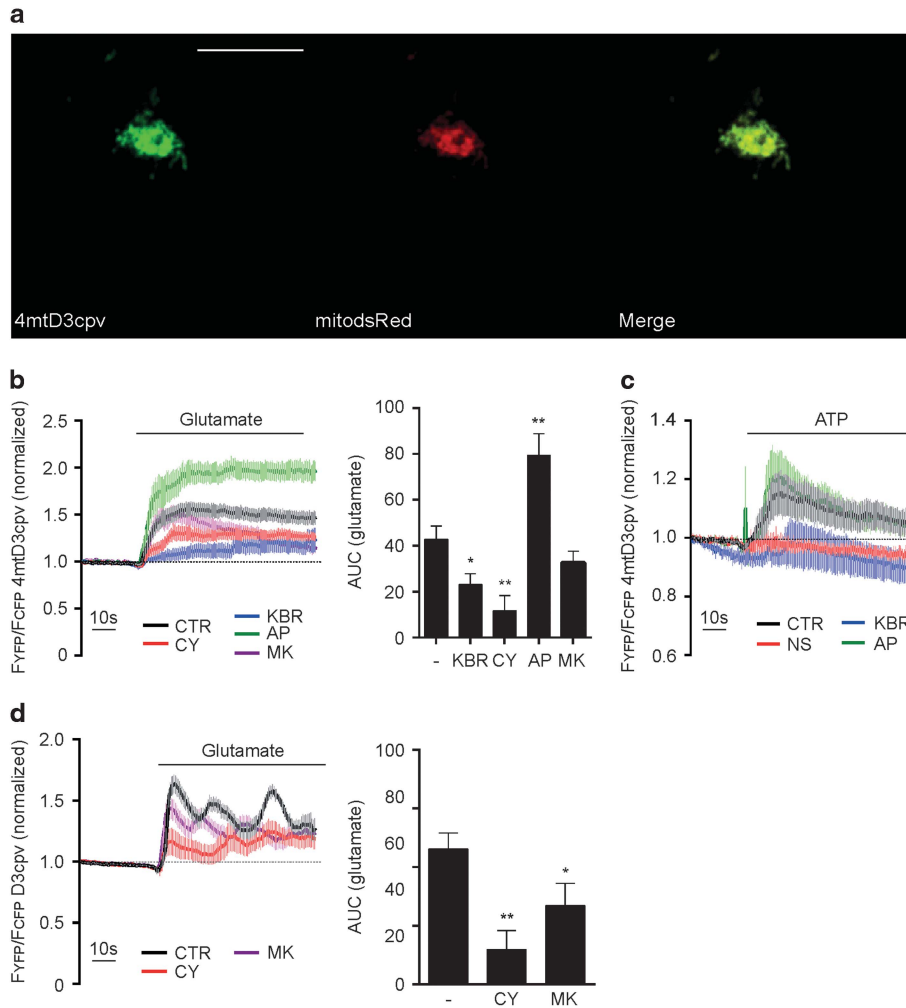


**Figure 7** SK channel activation reduces mitochondrial calcium uptake in PCN. (a) Representative confocal images of PCN expressing the FRET sensor and mitochondrial dsRed (mitodsRed). Scale bar: 10  $\mu$ m,  $n = 5$ . (b) FRET recordings of PCN expressing 4mtD3cpv following glutamate stimulation. Left panel: FRET traces after pre-treatment with CyPPA (CY; red line), KB-R7943 (KBR; blue line), apamin (AP; green line) and MK801 (MK; purple line). Each trace was normalized to the initial value. Right panel: quantification of FRET recordings as area under curve after glutamate stimulation. Data are shown as mean  $\pm$  SEM,  $n = 8-20$ . \* $P < 0.05$ , \*\* $P < 0.01$  compared to control. (c) FRET recordings of PCN expressing 4mtD3cpv following ATP stimulation after pre-treatment with NS309 (NS; red line), KB-R7943 (KBR; blue line) and apamin (AP; green line) following ATP stimulation. Each trace was normalized to the initial value. Data are shown as mean  $\pm$  SEM,  $n = 8-20$ . \* $P < 0.05$ , \*\* $P < 0.01$  compared to control. (d) FRET recordings of PCN expressing D3cpv following glutamate stimulation after pre-treatment with CyPPA (CY; red line) or MK801 (MK; purple line). Each trace was normalized to the initial value. Data are shown as mean  $\pm$  SEM,  $n = 10-15$ . \* $P < 0.05$ , \*\* $P < 0.01$  compared to control

Taken together, our study reveals that the activation of mitochondrial SK2 channels determines protection against oxidative stress-induced cell death by preventing mitochondrial dysfunction. In particular, SK channel activation and mitoSK2 overexpression preserved cell viability, and reduced MMP loss and the formation of mitochondrial ROS through a mechanism involving attenuation of mitochondrial respiration and  $[Ca^{2+}]_m$  uptake.

#### Materials and methods

**Cell culture.** HT22 cells were cultured in Dulbecco's modified Eagle Medium (DMEM; Sigma Aldrich, Munich, Germany) supplemented with 10% fetal calf serum (FCS; PAA Cölbe, Germany), 100 U/ml penicillin, 100  $\mu$ g/ml streptomycin, and 2 mM L-glutamine (Invitrogen, Karlsruhe, Germany) at 37  $^{\circ}$ C and 5% CO<sub>2</sub>. Primary rat cortical neurons (PCN) were cultured on PEI-coated 24 mm coverslips in neurobasal medium (PAA, Cölbe, Germany) supplemented with 100 U/ml penicillin, 100  $\mu$ g/ml streptomycin, 2 mM L-glutamine and 2% B27 supplement (Gibco, Life

technologies, Darmstadt, Germany). SK2 channels were pharmacologically activated with the selective SK2/SK3 channel activator N-Cyclohexyl-N-[2-(3,5-dimethyl-pyrazol-1-yl)-6-methyl-4-pyrimidinamine (CyPPA; Sigma Aldrich, Munich, Germany)<sup>54</sup> and inhibited with the bee venom toxin apamin (Sigma Aldrich, Munich, Germany).<sup>33</sup>

**Plasmid transfection.** HT22 cells were transfected with control plasmids (pEGFP (GFP) or AAV2-CMV-2xMTS-eGFP (mitoGFP)), non-targeted and targeted SK2 channel plasmids (pEGFP-SK2 (SK2) or pEGFP-2xMTS-SK2 (mitoSK2)) or dominant-negative SK2 channel plasmids (pEGFP-SK2 DN (SK2 DN) or pEGFP-2xMTS-SK2 DN (mitoSK2 DN) using the attractene protocol (Qiagen, Hilden, Germany). MitoSK2 was generated by fusing the mitochondrial targeting sequence of cytochrome c at the N-terminus of SK2 on the plasmid twice. Due to a GYG-to-AAA mutation at amino acid positions 393-395 in the pore domain, the dominant-negative SK2 channel mutants have lost the ability to gate potassium. The transfection efficiency was quantified using FACS analysis. PCN (Div4-5) were transfected with 2  $\mu$ g of the cameleon FRET sensor (pcDNA-4mtD3cpv; Addgene, Cambridge, USA)<sup>44</sup> for 72-96 h using the lipofectamine2000 protocol (Thermo Fisher Scientific, Darmstadt, Germany).

**Confocal imaging.** HT22 cells ( $2.5 \times 10^4$  cells) were seeded onto 12 mm coverslips and transfected with control plasmids (GFP or mitoGFP), SK2 constructs (SK2 or mitoSK2), or dominant-negative SK2 constructs (SK2 DN or mitoSK2 DN) for 48 h. Mitochondria were stained with 200 nM MitoTracker Deep Red (Thermo Fisher Scientific, Darmstadt, Germany) for 30 min at 37 °C. PCN ( $2.5 \times 10^5$  cells) were cultivated on a PEI-coated 24well plate for 96 h and transfected with pcDNA-4mtD3cpv and mitorRed (Addgene, Cambridge, USA) for 7–96 h. Coverslips were fixed with 4% paraformaldehyde for 25 min at room temperature and mounted onto glass slides using Aqua-Poly/Mount (Polysciences, Eppelheim, Germany). Confocal images were acquired using a Leica SP5 microscope at 64x magnification. Image overlays were done using the ImageJ software.

**Cell viability assays.** HT22 cells were transfected with GFP control or SK2 channel plasmid in a 96well plate. Cell viability was assessed in real-time using the xCELLigence system (Roche, Munich, Germany) with cellular impedance measured every 30 min and represented as cellular index. Alternatively, cell viability was assessed by addition of 3-(4,5-dimethylthiazol-2-yl)-2,5-diphenyltetrazolium bromide (MTT) at a final concentration of 0.5 mg ml<sup>-1</sup> and incubation for 1 h at 37 °C. After removal of the medium and incubation at -80 °C, the resulting purple formazan was dissolved in DMSO. Absorbance was measured at 570 nm versus 630 nm with FluoStar Optima (BMG Labtech, Offenbach, Germany). For calcium chelation experiments, HT22 cells were treated with glutamate in the presence of EGTA (1 mM or 1.5 mM), in calcium-free or calcium-free medium supplemented with EGTA (0.25 mM). Cellular ATP levels as a measure of cell viability were determined using the ATP ViaLight Plus Kit (Lonza, Verviers, Belgium). After cell lysis for 10 min at 37 °C, 150 r.p.m., cellular ATP was detected by addition of the ATP monitoring reagent for 2 min at room temperature using the FluoStar Optima (BMG Labtech, Offenbach, Germany).

**Electrophysiology.**  $2.5 \times 10^4$  cells were seeded onto 12 mm coverslips, transfected with GFP, SK2 or SK2 DN and grown for 48 h. Electrophysiological recordings were performed at room temperature (20–22 °C). Whole-cell Voltage Clamp recordings of SK currents were performed with an EPC10 amplifier (HEKA). Patch pipettes were prepared from borosilicate glass capillaries GB 150TF-8P (Science Products, Hofheim, Germany), with tip resistances of 3–5 M $\Omega$ . Series resistance was compensated by 50%. The bath solution contained 130 mM NaCl, 5 mM KCl, 10 mM glucose, 1 mM MgCl<sub>2</sub>, 2 mM CaCl<sub>2</sub>, and 10 mM HEPES (pH7.4). The pipette solution contained 120 mM KCl, 2 mM MgCl<sub>2</sub>, 5 mM BAPTA, 4.43 mM CaCl<sub>2</sub> and 10 mM HEPES (pH7.3). The concentration of 1  $\mu$ M free Ca<sup>2+</sup> to fully activate SK currents was calculated using the program WINMAXC. Data were analyzed with ClampFit10 (Molecular Devices, Sunnyvale CA, USA). To measure SK channel-mediated currents, a voltage ramp protocol starting from a holding potential of -50 mV and subsequently depolarizing the membrane potential from -130 mV to +70 mV in 1000 ms was used. Data were analyzed with ClampFit10 (Molecular Devices, Sunnyvale CA, USA).

**High-resolution respirometry.** Mitochondrial respiration was analyzed by high-resolution respirometry using the oxygraph O2K (Oroboros systems, Innsbruck, Austria). Wildtype or transfected HT22 cells ( $5-9 \times 10^7$ ) were collected, and mitochondria were extracted using a pump-controlled system as described.<sup>55</sup> The mitochondrial respiration of 200  $\mu$ g crude mitochondria was monitored under continuous stirring at 750 rpm in 1 ml MiRO5 buffer (0.5 mM EGTA, 3 mM MgCl<sub>2</sub>, 60 mM lactobionic acid, 20 mM taurine, 10 mM KH<sub>2</sub>PO<sub>4</sub>, 20 mM HEPES, 110 mM D-Sucrose, BSA, 1 g/l essentially fatty acid free, at pH7.4). Oxygen polarography was performed at 37 °C and the oxygen flux per tissue mass (pmol O<sub>2</sub> s<sup>-1</sup> mg<sup>-1</sup>) were recorded in real-time using the DatLab software. Non-phosphorylating respiration or mitochondrial respiration state 2 was induced by adding the complex I-linked substrates pyruvate (5 mM), and malate (2 mM) (Figure 3a, state 2). Subsequently, the OXPHOS-capacity of complex I-linked activity or basal respiration (state 3) was measured after addition of a saturating concentration of ADP (0.8 mM). Afterwards, oligomycin (0.1  $\mu$ g/ml) was added to inhibit the ATP synthase. The maximum respiration (mitochondrial state 4u) was monitored by stepwise titration of the protonophore carbonyl cyanide 4-(trifluoromethoxy) phenylhydrazone (FCCP) in 1  $\mu$ M steps. The oxygen concentration and the first derivative of the oxygen concentration, reported as the oxygen consumption given in the O<sub>2</sub> slope (pmol x (ml/s)) of crude isolated mitochondria were recorded in 2 s intervals using instrumental background correction after calibration of the polarographic oxygen sensors.

**Measurement of mitochondrial calcium.** Changes in mitochondrial calcium were determined by the rhodamine-2-acetoxymethylester dye (Rho2-AM, Life Technologies). Cells were collected and incubated with 2  $\mu$ M dye in DMEM without serum for 25–30 min followed by incubation in DMEM for 25–30 min at room temperature in the dark. The fluorescence was excited at 552 nm and detected at 581 nm using the Guava Easy Cite 6-2L system (Merck Millipore, Darmstadt, Germany). Data were recorded from  $1 \times 10^4$  cells in triplicate per condition.

**Mitochondrial superoxide (ROS) formation.** Mitochondrial ROS formation was assessed by the MitoSOX dye (Invitrogen, Karlsruhe, Germany). Cells were incubated with 2.5  $\mu$ M MitoSOX dye for 30 min at 37 °C and collected afterwards. Fluorescence was excited at 488 nm and detected at 690/50 nm. Data were recorded from  $1 \times 10^4$  cells in triplicate per condition.

**Measurement of the mitochondrial membrane potential ( $\Delta\psi_m$ ).** Loss of the  $\Delta\psi_m$  was evaluated by staining with TMRE (tetramethylrhodamine-ethyl ester; Invitrogen, Karlsruhe, Germany) dye. Cells were collected and incubated 20 min with 0.2  $\mu$ M TMRE. TMRE fluorescence was excited at 488 nm and detected at 690/50 nm. Data were recorded from  $1 \times 10^4$  cells in triplicate per condition.

**Lipid peroxidation.** Lipid peroxidation was analyzed by staining with 2  $\mu$ M BODIPY dye (Invitrogen, Karlsruhe, Germany) for 60 min at 37 °C. A shift in BODIPY fluorescence from red to green was assessed by excitation at 488 nm and detection with a 525/30 nm band pass filter and a 690/50 nm band pass filter. Data were recorded from  $1 \times 10^4$  cells in triplicate per condition.

**Mitochondrial aequorin.** HT22 cells stably transfected with the mitochondrial apoprotein<sup>38</sup> of aequorin (HT22[mtAEQ]) were generated by viral transduction and kindly provided by Prof. Fabiana Perocchi. HT22[mtAEQ] cells ( $8 \times 10^4$  cells) were seeded into a white-walled 96well (Greiner Bioscience, Frickenhausen, Germany) and incubated for 24 h with SK channel modulators CyPPA (50  $\mu$ M), and apamin (1  $\mu$ M), the mNCLX inhibitor KB-R7943 (10  $\mu$ M),<sup>56</sup> antimycin A (50  $\mu$ M) or mitoK<sub>ATP</sub> inhibitors quinine (25  $\mu$ M) or glibenclamide (20  $\mu$ M) for 24 h. The cells were washed twice with modified Krebs Ringer Buffer (mKRB) containing 135 mM NaCl, 5 mM KCl, 0.4 mM KH<sub>2</sub>PO<sub>4</sub>, 20 mM HEPES and 5.5 mM glucose, and 1 mM CaCl<sub>2</sub>.<sup>38</sup> The active aequorin was reconstituted by incubation with 2.5  $\mu$ M coelenterazine (Biotium, VWR Technologies, Darmstadt, Germany) for 2 h at 37 °C. The basal luminescence signal was recorded followed by injection of 50  $\mu$ l calcium-perturbing agent (100  $\mu$ M ATP or 500  $\mu$ M carbachol) and final cell lysis with 1% Triton-X100/10 mM CaCl<sub>2</sub>. For the measurement, the FluoStar OPTIMA (BMG Labtech, Offenbach, Germany) was used. Each condition was recorded in triplicate and the peak amplitude was calculated for each treatment as percent of control.

**FRET-based calcium measurement.** Rat primary cortical neurons (Div6-8) (PCN) transfected with a mitochondrial (4mtD3cpv) or cytosolic (D3cpv) FRET sensor were maintained in pre-warmed buffer containing 137 mM NaCl, 5.4 mM KCl, 1 mM MgCl<sub>2</sub>, 10 mM HEPES, pH7.2, supplemented with 2 mM CaCl<sub>2</sub> and 1%BSA (Sigma Aldrich, Munich, Germany) at room temperature. [Ca<sup>2+</sup>]<sub>m</sub> uptake was induced by stimulation with 25  $\mu$ M glutamate or 100  $\mu$ M ATP after pre-incubation with SK channel modulators for 60–90 min. SK channels were activated with the SK2/SK3-specific activators CyPPA (50  $\mu$ M) or NS309 (50  $\mu$ M) and inhibited by the addition of apamin (1  $\mu$ M). KB-R7943 (10  $\mu$ M) was used as a positive control. PCN were analyzed at  $\times 100$  magnification in real-time using an inverted eclipse Ti Nikon microscope. CFP fluorescence was excited at 435 nm (430/24 filter, T455LP beam splitter). CFP and YFP fluorescence emission were collected using a CFP/YFP beam splitter ( $\lambda$  488/800-1064 rpc) and emission filters F480 (480/40) and F535 (535/30). The fluorescent signal was collected using a charge-coupled device camera (Evolve 512; Photometrics, Tucson, AZ). The FRET signal was calculated as the ratio of YFP fluorescence to CFP fluorescence ( $F_{YFP}/F_{CFP}$ ) including corrections for background, bleed through and photobleaching, and normalized to the initial measurement values. The exposure was set to 60–80 ms to avoid photobleaching. Triplicate recordings were performed for each condition. For comparative analysis, the area under curve was calculated.

**Statistical analysis.** Statistical significance was assessed using the unpaired Student's *t*-test or ANOVA and Scheffé's test for multiple comparisons, unless otherwise stated. *P* values indicating statistically significant differences between the mean values are defined as follows: \**P* < 0.05, \*\**P* < 0.01, and \*\*\**P* < 0.001.



## Conflict of Interest

The authors declare no conflict of interest.

**Acknowledgements.** We thank Katharina Elsässer for her excellent technical support and advice, and Emma Jane Esser for careful reading and correction of the manuscript. Further, we thank Prof Bernd Fakler for providing the SK2 channel plasmids, Susanne Michels for performing the MTT assays with MK801 and Maren Richter for providing fluorescence images of Rho2 distribution in HT22 cells. The work of FP was supported by the German Research Foundation (DFG) under the Emmy Noether Programme [PE 2053/1-1] and the Bavarian Ministry of Sciences, Research and the Arts in the framework of the Bavarian Molecular Biosystems Research Network [D2-F5121.2-10c/4822]. This work was supported by a grant from the Deutsche Forschungsgemeinschaft, DFG (DO 1525/3-1) and, in parts, by the von-Behring-Röntgen Stiftung. AMD is the recipient of a Rosalind Franklin Fellowship co-funded by European Union and University of Groningen.

## Author contributions

BH, LeM and TM carried out the experiments and performed data analysis. AMD, CC and BH participated in the design of the study and wrote the manuscript. LiM and ND designed, performed and analyzed patch clamp experiments. GKG, AG, BMB, CK and MB provided insightful discussions and contributed to data analysis. HZ, FP, AG and SS provided methods, cells and plasmids. All authors read and approved the final manuscript.

- Rizzuto R, De Stefani D, Raffaello A, Mammucari C. Mitochondria as sensors and regulators of calcium signalling. *Nat Rev Mol Cell Biol* 2012; **13**: 566–578.
- Wang L, Yang X, Shen Y. Molecular control of mitochondrial calcium uptake. *Biochem Biophys Res Commun* 2014; **449**: 373–376.
- McCormack JG, Denton RM. The effects of calcium ions and adenine nucleotides on the activity of pig heart 2-oxoglutarate dehydrogenase complex. *Biochem J* 1979; **180**: 533–544.
- Maeda N, Kawasaki T, Nakade S, Yokotag N, Taguchi T, Kasai M, Mikoshiba M. Structural and functional characterization of inositol 1,4,5-trisphosphate receptor channel from mouse cerebellum. *J Biol Chem* 1991; **266**: 1109–1116.
- Rizzuto R, Pinton P, Carrington W, Fay F, Fogarty K, Lifshitz L et al. Close contacts with the endoplasmic reticulum as determinants of mitochondrial Ca<sup>2+</sup> responses. *Science* 1998; **280**: 1763–1766.
- Joseph JA, Strain JG, Jimenez ND, Fisher D. Oxidant injury in PC12 cells—a possible model of calcium ‘dysregulation’ in aging: II. Interactions with membrane lipids. *J Neurochem* 1997; **69**: 1259–1266.
- Zündorf G, Reiser G. Calcium dysregulation and homeostasis of neural calcium in the molecular mechanisms of neurodegenerative diseases provide multiple targets for neuroprotection. *Antioxid Redox Signal* 2011; **14**: 1275–1288.
- Hoth M, Button DC, Lewis RS. Mitochondrial control of calcium-channel gating: a mechanism for sustained signaling and transcriptional activation in T lymphocytes. *Proc Natl Acad Sci* 2000; **97**: 10607–10612.
- Pacher P, Hajnóczky G. Propagation of the apoptotic signal by mitochondrial waves. *EMBO J* 2001; **20**: 4107–4121.
- Szalai G, Krishnamurthy R, Hajnóczky G. Apoptosis driven by IP<sub>3</sub>-linked mitochondrial calcium signals. *EMBO J* 1999; **18**: 6349–6361.
- Lemasters J, Theruvath T, Zhong Z, Nieminen A. Mitochondrial calcium and the permeability transition in cell death. *Biochim Biophys Acta* 2010; **1787**: 1395–1401.
- Chacon E, Acosta D. Mitochondrial regulation of superoxide for the cardiotoxicity by Ca<sup>2+</sup>: an alternate of doxorubicin mechanism. *Toxicol Appl Pharmacol* 1991; **128**: 117–128.
- Shutov LP, Kim M-S, Houlihan PR, Medvedeva YV, Usachev YM. Mitochondria and plasma membrane Ca<sup>2+</sup>-ATPase control presynaptic Ca<sup>2+</sup> clearance in capsaicin-sensitive rat sensory neurons. *J Physiol* 2013; **591**: 2443–2462.
- Young KW, Bampton ETW, Pinòn L, Bano D, Nicotera P. Mitochondrial Ca<sup>2+</sup> signalling in hippocampal neurons. *Cell Calcium* 2008; **43**: 296–306.
- De Stefani D, Bononi A, Romagnoli A, Messina A, De Pinto V, Pinton P et al. VDAC1 selectively transfers apoptotic Ca<sup>2+</sup> signals to mitochondria. *Cell Death Differ* 2012; **19**: 267–273.
- Pan X, Liu J, Nguyen T, Liu C, Sun J, Teng Y et al. The physiological role of mitochondrial calcium revealed by mice lacking the mitochondrial calcium uniporter. *Nat Cell Biol* 2013; **15**: 1464–1472.
- Perocchi F, Gohil V, Gargis H, Bao X, McCombs J, Palmer A et al. MICU1 encodes a mitochondrial EF hand protein required for Ca<sup>2+</sup> uptake. *Nature* 2010; **467**: 291–296.
- Qiu J, Tan Y, Hagenston A, Martel M, Kneisel N, Skehel P et al. Mitochondrial calcium uniporter Mcu controls excitotoxicity and is transcriptionally repressed by neuroprotective nuclear calcium signals. *Nat Commun* 2013; **4**: 2034.

- Stowe DF, Gadicherla AK, Zhou Y, Aldakkak M, Cheng Q, Kwok WM et al. Protection against cardiac injury by small Ca<sup>2+</sup>-sensitive K<sup>+</sup> channels identified in guinea pig cardiac inner mitochondrial membrane. *Biochim Biophys Acta* 2013; **1828**: 427–442.
- Dolga A, de Andrade A, Meissner L, Knaus H, Höllerhage M, Christophersen P et al. Subcellular expression and neuroprotective effects of SK channels in human dopaminergic neurons. *Cell Death Dis* 2014; **5**: e999.
- Dolga A, Netter M, Perocchi F, Doti N, Meissner L, Tobaben S et al. Mitochondrial small conductance SK2 channels prevent glutamate-induced oxytosis and mitochondrial dysfunction. *J Biol Chem* 2013; **288**: 10792–10804.
- Kuiper E, Nelemans A, Luiten P, Nijholt I, Dolga A, Eisel U. Kca2 and Kca3 channels in learning and memory processes, and neurodegeneration. *Front Pharmacol* 2012; **3**: 1–13.
- Cui M, Qin G, Zhang M, Yu K, Bowers MS. Targeting the Small- and Intermediate-Conductance Ca<sup>2+</sup>-activated potassium channels: the drug-binding pocket at the channel/calmodulin interface. *Neurosignals* 2014; **22**: 65–78.
- Skibbye L, Poulet C, Diness J, Bentzen B, Yuan L, Kappert U et al. Small-conductance calcium-activated potassium (SK) channels contribute to action potential repolarization in human atria. *Cardiovasc Res* 2014; **103**: 156–167.
- Richter M, Nickel C, Apel L, Kaas A, Dodel R, Culmsee C et al. (SK) channel activation modulates mitochondrial respiration and attenuates neuronal HT-22 cell damage induced by (H<sub>2</sub>O<sub>2</sub>). *Neurochem Int* 2015; **81**: 63–75.
- Richter M, Vidovic N, Honrath B, Mahavadi P, Dodel R, Dolga A, Culmsee C. Activation of SK2 channels preserves ER Ca<sup>2+</sup> homeostasis and protects against ER stress-induced cell death. *Cell Death Differ* 2015; **23**: 814–827.
- Dolga A, Terpolilli N, Kepura F, Nijholt IM, Knaus H, D’Orsi B et al. KCa2 channels activation prevents [Ca<sup>2+</sup>]<sub>i</sub> deregulation and reduces neuronal death following glutamate toxicity and cerebral ischemia. *Cell Death Dis* 2011; **2**: e147.
- Dolga AM, Culmsee C. Protective roles for potassium SK/Kca2 channels in microglia and neurons. *Front Pharmacol* 2012; **3**: 1–9.
- Allen D, Nakayama S, Kuroiwa M, Nakano T, Palmateer J, Kosaka Y et al. SK2 channels are neuroprotective for ischemia-induced neuronal cell death. *J Cereb Blood Flow Metab* 2011; **31**: 2302–2312.
- Wiczor B, Marcu R, Hawkins B. KB-R7943, a plasma membrane Na<sup>+</sup>/Ca<sup>2+</sup> exchanger inhibitor, blocks opening of the mitochondrial permeability transition pore. *Biochem Biophys Res Commun* 2013; **18**: 1199–1216.
- Murphy TH, Miyamoto M, Sastre A, Schnaar RL, Coyle JT. Glutamate toxicity in a neuronal cell line involves inhibition of cystine transport leading to oxidative stress. *Neuron* 1989; **2**: 1547–1558.
- Diemert S, Dolga A, Tobaben S, Grohm J, Pfeifer S, Oexler E, Culmsee C. Impedance measurement for real time detection of neuronal cell death. *J Neurosci Methods* 2012; **203**: 69–77.
- Deschaux O, Bizot JC. Effect of apamin, a selective blocker of Ca<sup>2+</sup>-activated K<sup>+</sup>-channel, on habituation and passive avoidance responses in rats. *Neurosci Lett* 1997; **227**: 57–60.
- Kroemer G, Galluzzi L, Brenner C. Mitochondrial Membrane Permeabilization in Cell Death. *Physiol Rev* 2007; **87**: 99–163.
- Tobaben S, Grohm J, Seiler A, Conrad M, Plesnila N, Culmsee C. Bid-mediated mitochondrial damage is a key mechanism in glutamate-induced oxidative stress and AIF-dependent cell death in immortalized HT-22 hippocampal neurons. *Cell Death Differ* 2011; **18**: 282–292.
- Seiler A, Schneider M, Förster H, Roth S, Wirth E, Culmsee C et al. Glutathione peroxidase 4 senses and translates oxidative stress into 12/15-Lipoxygenase dependent- and AIF-mediated cell death. *Cell Metab* 2008; **8**: 237–248.
- Rizzuto R, Simpson A, Brini M, Pozzan T. Rapid changes of mitochondrial Ca<sup>2+</sup> revealed by specifically targeted recombinant aequorin. *Nature* 1992; **356**: 133–135.
- Bonora M, Giorgi C, Bononi A, Marchi S, Patergnani S, Rimessi A et al. Subcellular calcium measurements in mammalian cells using jellyfish photoprotein aequorin-based probes. *Nat Protoc* 2013; **8**: 2105–2118.
- Santo-Domingo J, Vay L, Hernández-SanMiguel E, Lobatón CD, Moreno A, Montero M et al. The plasma membrane Na<sup>+</sup>/Ca<sup>2+</sup> exchange inhibitor KB-R7943 is also a potent inhibitor of the mitochondrial Ca<sup>2+</sup> uniporter. *Br J Pharmacol* 2007; **151**: 647–654.
- Medvedeva YV, Kim M-S, Usachev YM. Mechanisms of prolonged presynaptic Ca<sup>2+</sup> signaling and glutamate release induced by TRPV1 activation in rat sensory neurons. *J Neurosci* 2008; **28**: 311.
- Kuum M, Veksler V, Liiv J, Ventura-Clapier R, Kaasik A. Endoplasmic reticulum potassium-hydrogen exchanger and small conductance calcium-activated potassium channel activities are essential for ER calcium uptake in neurons and cardiomyocytes. *J Cell Sci* 2012; **125**: 625–633.
- Bednarczyk P, Kicińska A, Kominkova V, Ondrias K, Dolowy K, Szewczyk A. Quinine inhibits mitochondrial ATP-regulated potassium channel from bovine heart. *J Membr Biol* 2004; **199**: 63–72.
- Li DL, Ma ZY, Fu ZJ, Ling MY, Yan CZ, Zhang Y. Glibenclamide decreases ATP-induced intracellular calcium transient elevation via inhibiting reactive oxygen species and mitochondrial activity in macrophages. *PLoS ONE* 2014; **9**: e89083.
- Palmer AE, Tsien RY. Measuring calcium signaling using genetically targetable fluorescent indicators. *Nat Protoc* 2006; **1**: 1057–1065.
- Whitaker M. Genetically-encoded probes for measurement of intracellular calcium. *Methods Cell Biol* 2010; **99**: 153–182.



46. Öxler EM, Dolga A, Culmsee C. AIF depletion provides neuroprotection through a preconditioning effect. *Apoptosis* 2012; **17**: 1027–1038.
47. Schauen M, Spitzkovsky D, Schubert J, Fischer J, Hayashi J, Wiesner R. Respiratory chain deficiency slows down cell-cycle progression via reduced ROS generation and is associated with a reduction of p21 CIP1/WAF1. *J Cell Physiol* 2006; **207**: 12–22.
48. Dolga A, Granic I, Blank T, Knaus H, Spiess J, Luiten P et al. TNF- $\alpha$  mediates neuroprotection against glutamate-induced excitotoxicity via NF- $\kappa$ B-dependent up-regulation of K Ca 2.2 channels. *J Neurochem* 2008; **107**: 1158–1167.
49. Hung CHL, Ho YS, Chang RCC. Modulation of mitochondrial calcium as a pharmacological target for Alzheimer's disease. *Ageing Res Rev* 2010; **9**: 447–456.
50. Chalmers S, McCarron JG. The mitochondrial membrane potential and Ca<sup>2+</sup> oscillations in smooth muscle. *J Cell Sci* 2008; **121**: 75–85.
51. Stowe DF, Aldakkak M, Camara AKS, Riess ML, Heinen A, Varadarajan S et al. Cardiac mitochondrial preconditioning by Big Ca<sup>2+</sup>-sensitive K<sup>+</sup> channel opening requires superoxide radical generation. *Am J Physiol Heart Circ Physiol* 2006; **290**: H434–H440.
52. Testai L, Martelli A, Marino A, D'Antongiovanni V, Ciregia F, Giusti L et al. The activation of mitochondrial BK potassium channels contributes to the protective effects of naringenin against myocardial ischemia/reperfusion injury. *Biochem Pharmacol* 2013; **85**: 1634–1643.
53. De Marchi U, Sassi N, Fioretti B, Catacuzzeno L, Cereghetti GM, Szabó I, Zoratti M. Intermediate conductance Ca<sup>2+</sup>-activated potassium channel (KCa3.1) in the inner mitochondrial membrane of human colon cancer cells. *Cell Calcium* 2009; **45**: 509–516.
54. Hougaard C, Eriksen BL, Jørgensen S, Johansen TH, Dyhring T, Madsen L et al. Selective positive modulation of the SK3 and SK2 subtypes of small conductance Ca<sup>2+</sup>-activated K<sup>+</sup> channels. *Br J Pharmacol Pharmacol* 2007; **151**: 655–665.
55. Schmitt S, Eberhagen C, Weber S, Aichler M, Zischka H. Isolation of mitochondria from cultured cells and liver tissue biopsies for molecular and biochemical analyses. *Proteom Profiling: Methods Protocols* 2015; **1295**: 87–97.
56. Iwamoto T, Watano T, Shigekawa M. A novel isothiourea derivative selectively inhibits the reverse mode of Na<sup>+</sup>/Ca<sup>2+</sup> exchange in cells expressing NCX1. *J. Biol. Chem.* 1996; **271**: 22391–22397.

Supplementary Information accompanies this paper on Cell Death and Differentiation website (<http://www.nature.com/cdd>)